NASA/TM—2002-212010 AIAA–2003–0883

A New Domain Decomposition Approach for the Gust Response Problem

James R. Scott
Glenn Research Center, Cleveland, Ohio

Hafiz M. Atassi and Romeo F. Susan-Resiga
University of Notre Dame, Notre Dame, Indiana

December 2002

The NASA STI Program Office . . . in Profile

Since its founding, NASA has been dedicated to the advancement of aeronautics and space science. The NASA Scientific and Technical Information (STI) Program Office plays a key part in helping NASA maintain this important role.

The NASA STI Program Office is operated by Langley Research Center, the Lead Center for NASA's scientific and technical information. The NASA STI Program Office provides access to the NASA STI Database, the largest collection of aeronautical and space science STI in the world. The Program Office is also NASA's institutional mechanism for disseminating the results of its research and development activities. These results are published by NASA in the NASA STI Report Series, which includes the following report types:

- TECHNICAL PUBLICATION. Reports of completed research or a major significant phase of research that present the results of NASA programs and include extensive data or theoretical analysis. Includes compilations of significant scientific and technical data and information deemed to be of continuing reference value. NASA's counterpart of peer-reviewed formal professional papers but has less stringent limitations on manuscript length and extent of graphic presentations.

- TECHNICAL MEMORANDUM. Scientific and technical findings that are preliminary or of specialized interest, e.g., quick release reports, working papers, and bibliographies that contain minimal annotation. Does not contain extensive analysis.

- CONTRACTOR REPORT. Scientific and technical findings by NASA-sponsored contractors and grantees.

- CONFERENCE PUBLICATION. Collected papers from scientific and technical conferences, symposia, seminars, or other meetings sponsored or cosponsored by NASA.

- SPECIAL PUBLICATION. Scientific, technical, or historical information from NASA programs, projects, and missions, often concerned with subjects having substantial public interest.

- TECHNICAL TRANSLATION. English-language translations of foreign scientific and technical material pertinent to NASA's mission.

Specialized services that complement the STI Program Office's diverse offerings include creating custom thesauri, building customized databases, organizing and publishing research results . . . even providing videos.

For more information about the NASA STI Program Office, see the following:

- Access the NASA STI Program Home Page at ***http://www.sti.nasa.gov***

- E-mail your question via the Internet to help@sti.nasa.gov

- Fax your question to the NASA Access Help Desk at 301–621–0134

- Telephone the NASA Access Help Desk at 301–621–0390

- Write to:
  NASA Access Help Desk
  NASA Center for AeroSpace Information
  7121 Standard Drive
  Hanover, MD 21076

NASA/TM—2002-212010 AIAA–2003–0883

A New Domain Decomposition Approach for the Gust Response Problem

James R. Scott
Glenn Research Center, Cleveland, Ohio

Hafiz M. Atassi and Romeo F. Susan-Resiga
University of Notre Dame, Notre Dame, Indiana

Prepared for the
41st Aerospace Sciences Meeting and Exhibit
sponsored by the American Institute of Aeronautics and Astronautics
Reno, Nevada, January 6–9, 2003

National Aeronautics and
Space Administration

Glenn Research Center

December 2002

The Aerospace Propulsion and Power Program at
NASA Glenn Research Center sponsored this work.

Available from

NASA Center for Aerospace Information
7121 Standard Drive
Hanover, MD 21076

National Technical Information Service
5285 Port Royal Road
Springfield, VA 22100

Available electronically at http://gltrs.grc.nasa.gov

A NEW DOMAIN DECOMPOSITION APPROACH FOR THE GUST RESPONSE PROBLEM

James R. Scott*
National Aeronautics and Space Administration
Glenn Research Center
Cleveland, Ohio 44135

Hafiz M. Atassi† and Romeo F. Susan-Resiga‡
University of Notre Dame
Notre Dame, Indiana 46556

Abstract

A domain decomposition method is developed for solving the aerodynamic/aeroacoustic problem of an airfoil in a vortical gust. The computational domain is divided into inner and outer regions wherein the governing equations are cast in different forms suitable for accurate computations in each region. Boundary conditions which ensure continuity of pressure and velocity are imposed along the interface separating the two regions. A numerical study is presented for reduced frequencies ranging from 0.1 to 3.0. It is seen that the domain decomposition approach is far superior to the conventional single domain approach in providing robust and grid independent solutions.

I. Introduction

Many flow fields that occur in aerospace applications involve upstream flow disturbances which propagate downstream, interact with structural components, and radiate sound. Typical examples include turbulent flow past a wing, unsteady flow around a propeller blade, and unsteady flow through a row of stator blades.

The governing equations for such flows are the unsteady Navier-Stokes equations. However, viscous effects are often confined to small regions of the flow, and the unsteady Euler equations can be solved instead. If one further assumes that the convected disturbances are not too large, and that the flow moves at high speed, then one can invoke the "rapid distortion"[1,2] approximation and solve the linearized unsteady Euler equations. In this case, one obtains the zeroth-order steady mean flow first, and then obtains the unsteady flow as a first-order perturbation.

When the mean flow is both inviscid and irrotational, the steady velocity can be expressed as the gradient of a potential, and the problem for determining the unsteady flow can be reduced to solving a single convective wave equation with a dipole source term. This was first shown by Goldstein[3], who decomposed the unsteady velocity into the sum of a potential component $\vec{\nabla}\phi$, and a vortical component $\vec{u}^{(I)}$, so that $\vec{u}(\vec{x},t) = \vec{\nabla}\phi + \vec{u}^{(I)}$. $\vec{u}^{(I)}$ is a known function of the upstream velocity disturbances and the mean flow Lagrangian coordinates. ϕ satisfies

$$\frac{D_0}{Dt}\left(\frac{1}{{c_0}^2}\frac{D_0\phi}{Dt}\right) - \frac{1}{\rho_0}\vec{\nabla}\cdot(\rho_0\vec{\nabla}\phi) = \frac{1}{\rho_0}\vec{\nabla}\cdot(\rho_0\vec{u}^{(I)}),$$

where c_0 is the mean flow speed of sound, ρ_0 is the mean flow density, and $\frac{D_0}{Dt}$ is the convective derivative based on the mean flow velocity. The unsteady pressure is given by $p = -\rho_0\frac{D_0\phi}{Dt}$. Goldstein's formulation thus reduces the linearized Euler equations to a single convective wave equation.

For most aerodynamic flows, there will be a frontal stagnation point or line where the mean velocity vanishes and the Lagrangian coordinates become singular. In this case, $\vec{u}^{(I)}$ also becomes singular and remains so along the body surface. This makes it difficult to use Goldstein's formulation directly for numerical calculations, since the potential velocity component $\vec{\nabla}\phi$ must cancel the singular behavior of $\vec{u}^{(I)}$ to satisfy the impermeablity condition.

Atassi and Grzedzinski[4] proposed a modified splitting of the unsteady velocity which removes the singular and indeterminate character of the vortical velocity on the body surface. Here the unsteady velocity is decomposed into the sum of an unknown potential component $\vec{\nabla}\phi$, and a known vortical component $\vec{u}^{(R)}$, where $\vec{u}^{(R)}$ has zero normal and streamwise velocity components on the body surface. The potential ϕ satisfies Goldstein's convective wave equation with a modified source term,

$$\frac{D_0}{Dt}\left(\frac{1}{{c_0}^2}\frac{D_0\phi}{Dt}\right) - \frac{1}{\rho_0}\vec{\nabla}\cdot(\rho_0\vec{\nabla}\phi) = \frac{1}{\rho_0}\vec{\nabla}\cdot(\rho_0\vec{u}^{(R)}).$$

---

*Senior Research Scientist, Acoustics Branch, Senior Member, AIAA

†Viola D. Hank Professor, Department of Aerospace and Mechanical Engineering, Fellow, AIAA

‡Visiting Associate Professor, Department of Aerospace and Mechanical Engineering

The surface boundary condition for ϕ is no longer singular and is in fact just $\vec{\nabla}\phi \cdot \vec{n} = 0$.

In a series of papers[5–10], Scott and Atassi presented the first numerical implementation of Atassi and Grzedzinski's linearized formulation for the case of unsteady vortical flow past a single airfoil. The main objective in this effort was to develop an aerodynamic solver, the GUST3D code, which could accurately predict the airfoil unsteady response to three-dimensional, periodic vortical gusts.

Another series of papers[11–15] focused on the far-field aeroacoustic response. It was noted in these papers that, although the GUST3D code produced an accurate near-field solution, there was a significant loss of accuracy in the far field. As a result, these papers concentrated on the development of Kirchoff methods to extend the GUST3D mid-field solution to the far field. Comparison of Kirchoff results with analytical solutions showed this to be a promising approach.

Building on this work, Scott[16] presented a series of benchmark solutions for CAA code validation at the recent Third Computational Aeroacoustics Workshop on Benchmark Problems. Comparison with results from nonlinear time-marching codes[16–21] showed good agreement on the airfoil surface and good agreement in the far field for low reduced frequencies. However, there were some discrepancies in the high reduced frequency comparisons.

An extensive evaluation of the GUST3D code indicated that, as the reduced frequency increases, the source term calculated by the code grows rapidly in the far field and oscillates, making it difficult to obtain an accurate solution.

The purpose of this paper is to present a new domain decomposition approach which largely corrects this problem. The basic idea is to divide the flow field into inner and outer regions, and to use the Atassi-Grzedzinski formulation in the inner region and the Goldstein formulation in the outer region. It will be seen that this approach leads to substantial improvements in accuracy, both on the airfoil and in the far field.

II. Mathematical Formulation

Governing Equations

Consider an airfoil with chord length c in a flow with uniform upstream velocity U_∞ in the x_1 direction. Let the fluid be an ideal gas which is inviscid and non-heat-conducting. Far upstream, let

$$\vec{u}_\infty = \vec{a}\, e^{i\vec{k}\cdot(\vec{x}-\vec{\imath}U_\infty t)} \tag{2.1}$$

denote a small amplitude gust, where $\vec{\imath}$ is a unit vector in the x_1 direction. Here $\vec{a} = (a_1, a_2, a_3)$, where the amplitude $|\vec{a}|$ satisfies $|\vec{a}| << U_\infty$, $\vec{k} = (k_1, k_2, k_3)$ is the wave number vector, and $\vec{a}$ and $\vec{k}$ satisfy $\vec{a}\cdot\vec{k} = 0$ to ensure that the continuity equation is satisfied.

Let the flow field be represented by

$$\vec{U}(\vec{x},t) = \vec{U}_0(\vec{x}) + \vec{u}(\vec{x},t) \tag{2.2}$$

$$p(\vec{x},t) = p_0(\vec{x}) + p'(\vec{x},t) \tag{2.3}$$

$$\rho(\vec{x},t) = \rho_0(\vec{x}) + \rho'(\vec{x},t) \tag{2.4}$$

$$s(\vec{x},t) = s_0 + s'(\vec{x},t) \tag{2.5}$$

where the entropy s_0 is constant, and $\vec{u}$, p', ρ', and s' are the unsteady perturbation velocity, pressure, density and entropy, respectively. Quantities with "$_0$" subscripts are the steady mean flow quantities which are assumed to be known.

Substituting (2.2) – (2.5) into the nonlinear Euler equations and neglecting products of small quantities, one obtains the linearized continuity, momentum, and entropy conservation equations

$$\frac{D_0\rho'}{Dt} + \rho'\vec{\nabla}\cdot\vec{U}_0 + \vec{\nabla}\cdot(\rho_0\vec{u}) = 0 \tag{2.6}$$

$$\rho_0\left(\frac{D_0\vec{u}}{Dt} + \vec{u}\cdot\vec{\nabla}\vec{U}_0\right) + \rho'\vec{U}_0\cdot\vec{\nabla}\vec{U}_0 = -\vec{\nabla}p' \tag{2.7}$$

$$\frac{D_0 s'}{Dt} = 0, \tag{2.8}$$

where $\frac{D_0}{Dt} = \frac{\partial}{\partial t} + \vec{U}_0\cdot\vec{\nabla}$.

Let the flow field be divided into inner and outer regions, as shown in Figure 1. In the outer region, let the unsteady velocity be decomposed according to Goldstein's velocity splitting,

$$\vec{u}(\vec{x},t) \;=\; \vec{\nabla}\phi_O + \vec{u}^{(G)}, \tag{2.9}$$

where we define $\vec{u}^{(G)} = \vec{u}^{(I)}$, and where the "$_O$" subscript denotes the outer region. Equations (2.6) - (2.8) are then reduced to

$$\mathcal{L}\,\phi_O \;=\; \frac{1}{\rho_0}\vec{\nabla}\cdot(\rho_0\vec{u}^{(G)}) \tag{2.10}$$

where

$$\mathcal{L} \;=\; \frac{D_0}{Dt}\left(\frac{1}{{c_0}^2}\frac{D_0}{Dt}\right) \;-\; \frac{1}{\rho_0}\vec{\nabla}\cdot(\rho_0\vec{\nabla}). \tag{2.11}$$

The unsteady pressure is given by

$$p' \;=\; -\rho_0\frac{D_0\,\phi_O}{Dt}. \tag{2.12}$$

In the inner region, let the velocity be decomposed according to the Atassi-Grzedzinski velocity splitting,

$$\vec{u}(\vec{x},t) \;=\; \vec{\nabla}\phi_I + \vec{u}^{(R)}, \tag{2.13}$$

where the "I" subscript denotes the inner region. Equations (2.6) - (2.8) then reduce to

$$\mathcal{L}\,\phi_I \;=\; \frac{1}{\rho_0}\vec{\nabla}\cdot(\rho_0\vec{u}^{(R)}). \tag{2.14}$$

For flows with no upstream entropy disturbances, $\vec{u}^{(R)}$ and $\vec{u}^{(G)}$ are related by[4]

$$\vec{u}^{(R)} \;=\; \vec{u}^{(G)} \;+\; \vec{\nabla}\tilde{\phi}, \tag{2.15}$$

where $\tilde{\phi}$ is a function which is constructed to cancel the singularity in $\vec{u}^{(G)}$ on the airfoil surface, so that ϕ_I has a regular boundary condition. It should be noted that $\tilde{\phi}$ has no pressure associated with it, so that the unsteady pressure in the inner region is just

$$p' \;=\; -\rho_0\frac{D_0\,\phi_I}{Dt}. \tag{2.16}$$

Boundary Conditions

At the airfoil surface, the normal velocity component must vanish. Since $\vec{u}^{(R)}$ has zero normal and streamwise velocity components along the airfoil surface, the airfoil boundary condition is just

$$\vec{\nabla}\phi_I\cdot\vec{n} = 0. \tag{2.17}$$

Across the wake, in both the inner and outer regions, the pressure and normal velocity must be continuous. For the pressure, this leads to

$$p'_+ \;-\; p'_- \;=\; -\rho_0\frac{D_0\big(\phi_+ \;-\; \phi_-\big)}{Dt} \;=\; 0, \tag{2.18}$$

where "+" and "-" subscripts denote quantities above and below the wake, respectively. (The inner and outer subscripts are omitted here for simplicity.) The inner and outer potentials must then satisfy

$$\frac{D_0\big(\triangle\,\phi\big)}{Dt} \;=\; 0, \tag{2.19}$$

where $\triangle\,\phi$ denotes the jump in ϕ across the wake. For continuity of normal velocity, the potentials must satisfy

$$\vec{\nabla}\phi_+\cdot\vec{n} \;=\; \vec{\nabla}\phi_-\cdot\vec{n}. \tag{2.20}$$

On the outer grid boundary, a radiation boundary condition must be imposed. This will be discussed in the next section.

Finally, interface conditions must be specified at the boundary separating the inner and outer regions. Analogous to the wake, the pressure and velocity should be continuous. For the pressure, this requires that

$$\frac{D_0\,\phi_O}{Dt} \;=\; \frac{D_0\,\phi_I}{Dt}, \tag{2.21}$$

where the spatial derivatives in (2.21) are understood to be one-sided.

For the velocity, one uses (2.9) and (2.13) together with (2.15) to obtain

$$\vec{\nabla}\phi_O \;=\; \vec{\nabla}\phi_I \;+\; \vec{\nabla}\tilde{\phi}. \tag{2.22}$$

Taking the dot product of each term in (2.22) with the interface unit normal $\vec{n}$, one obtains the continuity of normal velocity condition

$$\vec{\nabla}\phi_O\cdot\vec{n} \;=\; \vec{\nabla}\phi_I\cdot\vec{n} \;+\; \vec{\nabla}\tilde{\phi}\cdot\vec{n}. \tag{2.23}$$

Alternatively, one can integrate (2.22) to obtain the jump condition

$$\phi_O \;-\; \phi_I \;=\; \tilde{\phi}. \tag{2.24}$$

The pressure and normal velocity conditions, equations (2.21) and (2.23), represent a consistent set of conditions for non-overlapping domain decomposition. Equation (2.23) is a Neumann condition, while equation (2.21) is a linear combination of Dirichlet and Neumann conditions. They always form a linearly independent and therefore robust set of interface conditions for domain decomposition.

On the other hand, at an interface location where the mean velocity becomes tangent to the interface, equations (2.21) and (2.24) may not be linearly independent. This could lead to difficulties for some interface configurations.

III. Numerical Implementation

For the most general case, in which the steady velocity $\vec{U}_0(\vec{x})$ varies spatially as a function of $\vec{x}$, the right hand sides of (2.10) and (2.14) are expressed as functions of the mean flow Lagrangian coordinates. One therefore introduces the variables $(X_1, X_2, X_3) = \vec{X}$, where

$$X_2 = \frac{\Psi_0}{\rho_\infty U_\infty} \tag{3.1}$$

and

$$X_3 = x_3, \tag{3.2}$$

where Ψ_0 is the stream function of the mean flow and x_3 is the spatial coordinate in the spanwise direction. The component X_1 is given by

$$X_1 = U_\infty\Delta, \tag{3.3}$$

where Δ is the Darwin-Lighthill "drift" function[22,23], which can be expressed in terms of Φ_0 and Ψ_0 as

$$\Delta = \frac{\Phi_0}{{U_\infty}^2} + \int_{-\infty}^{\Phi_0}\Big(\frac{1}{{U_0}^2} - \frac{1}{{U_\infty}^2}\Big)\,d\Phi_0. \tag{3.4}$$

The integration is carried out on $\Psi_0 =$ constant (i.e., a fixed streamline).

For flows with no upstream entropy fluctuations, Goldstein's vortical velocity may then be expressed as

$$\vec{u}^{(G)} = [\vec{\nabla}(\vec{a}\cdot\vec{X})]e^{i\vec{k}\cdot(\vec{X}-\vec{i}U_\infty t)}, \tag{3.5}$$

and the Atassi-Grzedzinski vortical velocity is

$$\vec{u}^{(R)} = [\vec{\nabla}(\vec{a}\cdot\vec{X})]e^{i\vec{k}\cdot(\vec{X}-\vec{i}U_\infty t)} + \vec{\nabla}\tilde{\phi}. \tag{3.6}$$

The function $\tilde{\phi}$ is constructed to cancel the singularity in $\vec{u}^{(G)}$ on the airfoil surface, and is given by[4]

$$\tilde{\phi} = \frac{i}{k_1}(a_1 + \frac{a_2k_1 - a_1k_2}{1 + ia_0U_\infty k_1}\frac{1-e^{-ik_2X_2}}{k_2})e^{i\vec{k}\cdot(\vec{X}-\vec{i}U_\infty t)}, \tag{3.7}$$

where

$$a_0 = -\left(\frac{\partial U_0}{\partial n}\right)_S^{-1}. \tag{3.8}$$

Here n denotes the direction of the outward unit normal, and S denotes the stagnation point near the airfoil leading edge.

Now from (3.5) and (2.1), one can show that as $x_1 \to -\infty$, $\vec{u}^{(G)} \to \vec{u}_\infty$. Since we must also have $\vec{u}(\vec{x},t) \to \vec{u}_\infty$ at upstream infinity, it follows that in the outer region ϕ_O must satisfy $\vec{\nabla}\phi_O \to 0$ as $x_1 \to -\infty$. This ensures that ϕ_O has outgoing wave behavior at infinity.

On the other hand, in the inner region, it follows from (2.1), (2.13) and (3.6) that ϕ_I must satisfy $\vec{\nabla}\phi_I \to -\vec{\nabla}\tilde{\phi}$ as one moves toward upstream infinity. It is necessary, therefore, to replace ϕ_I with a function whose gradient vanishes as $x_1 \to -\infty$. This will ensure that the new potential has outgoing wave behavior, and reduce any incompatibility across the interface separating the inner and outer regions.

Following the formulation presented in [7,10], we introduce the potential functions ϕ_1 and ϕ_2, where

$$\phi_I \;=\; \phi_1 \;-\; \phi_2, \tag{3.9}$$

and ϕ_2 is a known function which is constructed such that

$$|\phi_2 - \tilde{\phi}| \to 0 \qquad \text{as} \quad r \to \infty, \tag{3.10}$$

where r denotes polar distance. This ensures that $\vec{\nabla}\phi_1 \to 0$ in the far field.

Upon substituting (3.9) into (2.14), the inner governing equation becomes

$$\mathcal{L}\,\phi_1 \;=\; \frac{1}{\rho_0}\vec{\nabla}\cdot(\rho_0\vec{u}^{(R)}) \;+\; \mathcal{L}\,\phi_2, \tag{3.11}$$

where the right hand side consists of known functions. The governing equation in the outer region remains that given in (2.10)

Equations (2.10) and (3.11) are most conveniently solved in the frequency domain using the (Φ_0, Ψ_0) orthogonal curvilinear coordinate system, where Φ_0 and Ψ_0 are the mean flow potential and stream functions.

We now assume that all variables have been nondimensionalized as in [7,10]. The normalized wave number k_1 denotes the reduced frequency, and the free stream Mach number is denoted by M_∞. We transform into the frequency domain in the inner and outer regions using

$$\phi_1 = \varphi_I\, e^{-ik_1t + ik_3x_3} \tag{3.12}$$

and

$$\phi_O = \varphi_O\, e^{-ik_1t + ik_3x_3}. \tag{3.13}$$

Transformation into computational coordinates is then accomplished as follows. First, introduce Prandtl-Glauert coordinates (Φ,Ψ) by

$$\Phi = \Phi_0 \tag{3.14a}$$

$$\Psi = \beta_\infty\Psi_0, \tag{3.14b}$$

where $\beta_\infty = \sqrt{1-M_\infty^2}$. Then introduce new dependent variables ψ_I and ψ_O, where

$$\varphi_I = \psi_I\, e^{-iK_0\Phi} \tag{3.15}$$

$$\varphi_O = \psi_O\, e^{-iK_0\Phi} \tag{3.16}$$

and

$$K_0 = \frac{k_1M_\infty^2}{\beta_\infty^2}. \tag{3.17}$$

Finally, transform Φ and Ψ into computational coordinates using

$$\Phi = a^\star\cos(\pi\eta)\cosh(\pi\xi) \tag{3.18a}$$

$$\Psi = a^\star\sin(\pi\eta)\sinh(\pi\xi), \tag{3.18b}$$

where $a^\star$ is a known constant. The inner governing equation then becomes

$$-\beta_\infty^2\Big[\frac{\partial^2\psi_I}{\partial\eta^2} + \frac{\partial^2\psi_I}{\partial\xi^2} + J(\eta,\xi)\left(\frac{k_1^2M_\infty^2}{\beta_\infty^4} - \frac{k_3^2}{\beta_\infty^2}\right)\psi_I\Big]$$

$$+ A_1\,J(\eta,\xi)\,\psi_I + T_1\frac{\partial\psi_I}{\partial\xi} + T_2\frac{\partial\psi_I}{\partial\eta} + T_3\frac{\partial^2\psi_I}{\partial\xi^2}$$

$$+ T_4\frac{\partial^2\psi_I}{\partial\eta^2} + T_5\,\frac{\partial^2\psi_I}{\partial\eta\partial\xi} \;=\; S_I, \tag{3.19}$$

where J, A_1, and T_1 ... T_5 are known functions, and S_I is the source term. Similarly, the outer governing equation is

$$-\beta_\infty^2\Big[\frac{\partial^2\psi_o}{\partial\eta^2}+\frac{\partial^2\psi_o}{\partial\xi^2}+J(\eta,\xi)\Big(\frac{k_1^2M_\infty^2}{\beta_\infty^4}-\frac{k_3^2}{\beta_\infty^2}\Big)\psi_o\Big]$$

$$+A_1\,J(\eta,\xi)\,\psi_o+T_1\frac{\partial\psi_o}{\partial\xi}+T_2\frac{\partial\psi_o}{\partial\eta}+T_3\frac{\partial^2\psi_o}{\partial\xi^2}$$

$$+T_4\frac{\partial^2\psi_o}{\partial\eta^2}+T_5\,\frac{\partial^2\psi_o}{\partial\eta\partial\xi}\;=\;S_o. \qquad (3.20)$$

Equations (3.19) and (3.20) are implemented using nine-point central differencing which is second-order accurate. Each equation is imposed at interior grid points within its respective region.

At the interface separating the two regions, one must ensure that the pressure and velocity are continuous, as discussed in the previous section. This is accomplished by using a row of coincident grid points along the interface, with one set of points belonging to the inner region and the other set belonging to the outer region. (See Figures 2a and b.) Pressure continuity is satisfied by imposing condition (2.21). Velocity continuity is satisfied by imposing either (2.23) or (2.24). In calculations to date, conditions (2.23) and (2.24) have been found to give nearly identical results.

For wake grid points, continuity of pressure and normal velocity are enforced by way of equations (2.19) and (2.20). Equation (2.19) is imposed in integral form for every wake point on the upper side. Equation (2.20) is imposed using three-point, one-sided differencing for every wake point on the lower side.

On the outer grid boundary, we impose the Bayliss-Turkel[24] radiation boundary condition of order 1. This condition is applied to the unsteady pressure, and can be written

$$\Big(\frac{\partial}{\partial r}\;-\;B\Big)\Big(\frac{\partial}{\partial\Phi}\;-\;A\Big)\,\psi_o\;=\;0, \qquad (3.21)$$

where

$$A\;=\;\frac{ik_1}{\beta_\infty^2} \qquad (3.22)$$

and

$$B\;=\;i\,k\;-\;\frac{1}{2\,r}. \qquad (3.23)$$

Here k is the Helmholtz constant which is defined by

$$k^2\;=\;\Big(\frac{k_1M_\infty}{\beta_\infty^2}\Big)^2-\Big(\frac{k_3}{\beta_\infty}\Big)^2. \qquad (3.24)$$

Condition (3.21) has proven to be both accurate and computationally efficient[25].

IV. Numerical Results

In this section, we compare numerical results using the new domain decomposition approach versus the original single domain approach. All calculations are for a 12% thick, symmetric Joukowski airfoil in a 2-D gust propagating at 45^0, i.e., $k_2 = k_1$. The airfoil has zero degrees angle of attack and no mean loading. The Mach number is 0.5. We consider reduced frequency values $k_1 = 0.1$, 1.0, 2.0, and 3.0 (with normalization based on the half chord). The gust amplitude is taken to be 2% of the free stream velocity.

In the results that follow, we present RMS pressure on the airfoil surface and acoustic intensity in the far field. For each reduced frequency, we present results from a series of calculations on five different grids. Each grid differs only in the location of its outer grid boundary. The mesh spacing is the same for all five grids, with uniform η spacing and variable ξ spacing. The ξ spacing provides 24 points per gust wavelength. Our main objective is to assess the ability of each approach to give a consistent solution which does not depend on the outer grid boundary location.

Figures 3 and 4 show the RMS pressure on the airfoil surface for the low frequency case $k_1 = 0.1$. The legend at the top of the figure indicates the distance (in gust wavelengths) to the outer grid boundary for each grid. This is specified in terms of the GUST3D parameter "nwaves". The results in these figures show that the airfoil pressure is indeed grid independent for each approach.

Figures 5 and 6 show the corresponding acoustic intensity on a circle of radius two chord lengths, centered about the airfoil center. (This circle lies within the inner region for all results presented in this paper. In general, there is no relationship between the location of the circle and the location of the interface.) Each figure shows some sensitivity of the far-field pressure to the location of the outer grid boundary, with the domain decomposition results being slightly less sensitive.

We should note that the values of nwaves that were used in our calculations were designed to optimize accuracy for each reduced frequency and for each computational approach. All figures show results for five consecutive values of nwaves, where nwaves was incremented by 0.5. Each figure shows the best set of five consecutive results available for that case. This is the reason for the different values of nwaves that are shown.

In Figures 7-10, we present results for the mid-frequency case, $k_1 = 1.0$. Here the single domain results begin to show significant sensitivity to the change in grid, even on the airfoil surface. On the other hand, the domain decomposition results are very nearly grid independent on the airfoil and acceptably grid independent in the far field.

In Figures 11 - 18, we present results for the relatively high reduced frequencies of $k_1 = 2.0$ and $k_1 = 3.0$. At these higher frequencies, the single domain results deteriorate markedly due to the rapidly growing and oscillating source term, as shown in Figure 19. The domain decomposition results, however, give an acceptably grid independent solution both on the airfoil and in the far field.

We should point out, however, that the domain decomposition results are somewhat sensitive to the location of the interface separating the inner and outer regions, especially at high frequencies. We should note in addition that grid independence by itself does not imply accuracy. For this reason, the $k_1 = 2.0$ and $k_1 = 3.0$ results should be considered preliminary at this time.

Summary

In this paper we have presented a new domain decomposition approach for the single airfoil gust response problem. We divide the flow field into inner and outer regions, and use the Atassi-Grzedzinski linearized Euler formulation in the inner region, and Goldstein's linearized Euler formulation in the outer region. This approach uses each formulation where it is best suited. In the inner region, the Atassi-Grzedzinski formulation cancels the singularity in Goldstein's vortical velocity, and provides a boundary value problem with regular boundary conditions. In the outer region, far away from the airfoil singularity, Goldstein's formulation provides a boundary value problem which is better suited for wave propagation in an open domain. Numerical results show that the single domain approach is very sensitive to the location of the outer grid boundary, and is unable to provide a consistent or grid independent solution at the higher reduced frequencies. On the other hand, the domain decomposition approach is largely insensitive to the location of the outer grid boundary, and provides an acceptably grid independent solution for reduced frequencies ranging from 0.1 to 3.0.

References

1. Ribner, H. S. and Tucker, M., "Spectrum of Turbulence in a Contracting Stream," *NACA Report No. 1113, 1953.*
2. Batchelor, G. K. and Proudman, I., "The Effect of Rapid Distortion of a Fluid in Turbulent Motion," *Quart. J. Mech. Appl. Math. 1,* 1954, pp. 83-103.
3. Goldstein, M.E., "Unsteady vortical and entropic distortions of potential flows round arbitrary obstacles," *J. Fluid Mech.* **89**, 433-468, (1978).
4. Atassi, H.M. and Grzedzinski, J., "Unsteady disturbances of streaming motions around bodies," *J. Fluid Mech.* **209**, 385-403, (1989).
5. Atassi, H. M. and Scott, J. R., "Analysis of Nonuniform Subsonic Flows About a Row of Moving Blades," *Proceedings of the Fourth International Symposium on Unsteady Aerodynamics and Aeroelasticity of Turbomachines and Propellers,* H. E. Gallus and S. Servaty, eds., Institute fur Strahlantriebe und Turbomachine, University of Aachen, Federal Republic of Germany, 1988, pp. 39-67.
6. Scott, J. R. and Atassi, H. M., "Numerical Solution of Periodic Vortical Flows About a Thin Airfoil," AIAA Paper 89-1691, June, 1989.
7. Scott, J. R.,"Compressible Flows with Periodic Vortical Disturbances Around Lifting Airfoils," Ph.D. Dissertation, University of Notre Dame, April, 1990.
8. Scott, J.R. and Atassi, H.M., "Numerical Solutions of the Linearized Euler Equations for Unsteady Vortical Flows Around Lifting Airfoils," AIAA Paper 90-0694, January, 1990.
9. Scott, J.R. and Atassi, H.M., "High Frequency Gust Interaction with Single Loaded Airfoils in Subsonic Flows" *Proceedings of the Sixth International Symposium on Unsteady Aerodynamics, Aeroacoustics and Aeroelasticity of Turbomachines and Propellers*, University of Notre Dame, H.M. Atassi, ed., (Springer-Verlag, New York, 1991), 743-764.
10. Scott, J.R. and Atassi, H.M., "A Finite-Difference, Frequency-Domain Numerical Scheme for the Solution of the Gust Response Problem," *J. Comp. Phys.* **119**, 75-93, 1995.
11. Atassi, H.M., Subramaniam, S., and Scott, J.R., "Acoustic Radiation from Lifting Airfoils in Compressible Subsonic Flow," AIAA Paper 90-3911, October, 1990.
12. Atassi, H.M., Dusey, M., and Davis, C.M., "Acoustic Radiation from a Thin Airfoil in Nonuniform Subsonic Flows," *AIAA Journal*, Vol. 31, No. 1, pp. 12-19, 1993.
13. Patrick, S.M., Davis, C.M., and Atassi, H.M., "Acoustic Radiation from a Lifting Airfoil in Nonuniform Subsonic Flow," *ASME Computational Aero- and Hydro- Acoustics*, Vol. 147, pp. 41-46, 1993.
14. Atassi, H.M., Fang, J., and Patrick, S.M., "Direct Calculation of Sound Radiated From Bodies in Nonuniform Flows," *Journal of Fluids Engineering*, Vol. 115, pp. 573-579, 1993.
15. Hariharan, S., Scott, J.R., and Kreider, K.L., "A Potential-Theoretic Method for Far-Field Sound Radiation Calculations," *J. Comp. Phys.* **164**, pp. 143-164, 2000.
16. Third Computational Aeroacoustics (CAA) Workshop on Benchmark Problems, Proceedings of a conference held at and sponsored by Ohio Aerospace Institute, Cleveland, Ohio, Nov. 8-10, 1999, NASA/CP-2000-209790.
17. Hixon, R., Shih, S.-H., Mankbadi R.R., and Scott, J.R., "Time Domain Solution of the Airfoil Gust Problem Using a High-Order Compact Scheme," AIAA Paper 98-3241, 1998.

18. Hixon, R., Mankbadi R.R., and Scott, J.R., "Validation of a High-Order Prefactored Compact Code on Nonlinear Flows with Complex Geometries," AIAA Paper 2001-1103, January, 2001.
19. Rasetarinera, P., Kopriva, D.A., and Hussaini, M.Y., "Discontinuous Spectral Element Solution of Acoustic Radiation from Thin Airfoils," *AIAA Journal*, **39**, No. 11, 2070-2075, (2001).
20. Wang, X.Y., Chang, S.C., Himansu, A., and Jorgenson, P., "Gust Acoustic Response of a Single Airfoil Using the Space-Time CE/SE Method," AIAA Paper 2002-0801, January, 2002.
21. Crivellini, A., Golubev, V.V., Mankbadi R.R., Scott, J.R., Hixon, R., and Povinelli, L.A., "Nonlinear Analysis of Airfoil High-Intensity Gust Response Using a High-Order Prefactored Compact Code," AIAA Paper 2002-2535, June, 2002.
22. Darwin, C.G., *Proc. Cambridge Phil. Soc.*, **49**, 342, 1953.
23. Lighthill, M.J., *J. Fluid Mech.*, **1**, 31, 1956.
24. Bayliss, A. and Turkel, E., "Radiation boundary conditions for wave-like equations," *Comm. Pure Appl. Math.* **33**, 707-725 (1980).
25. Scott, J.R., Kreider, K.L., and Heminger, J.A., "Evaluation of Far-Field Boundary Conditions for the Gust Response Problem," AIAA Paper 2002-2441, June, 2002.

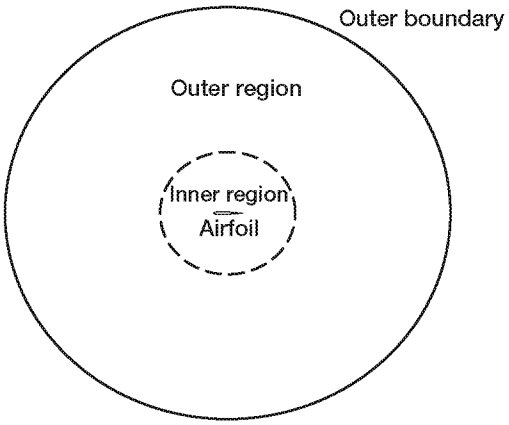

Figure 1.—Flow field with inner and outer regions.

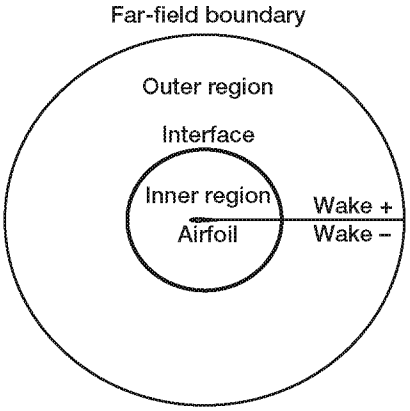

Figure 2(b).—Physical grid.

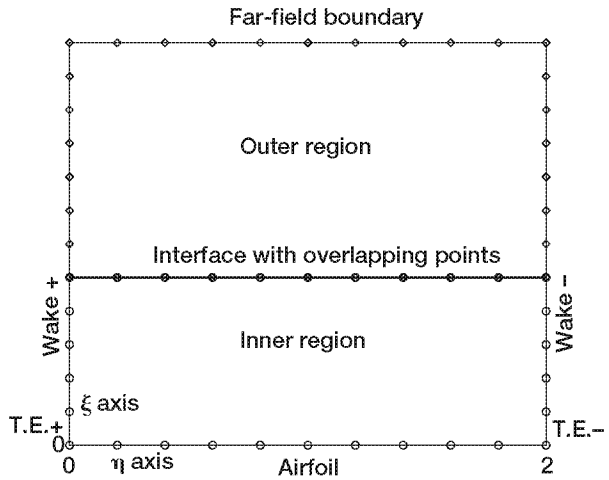

Figure 2(a).—Computational grid.

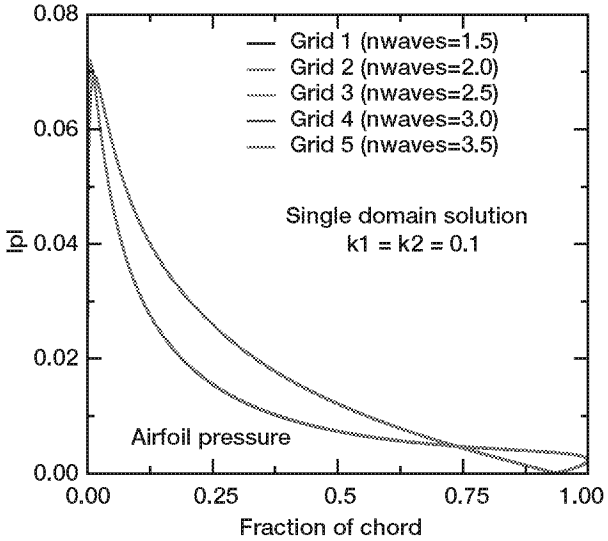

Figure 3.—Grid independent pressure on airfoil surface.

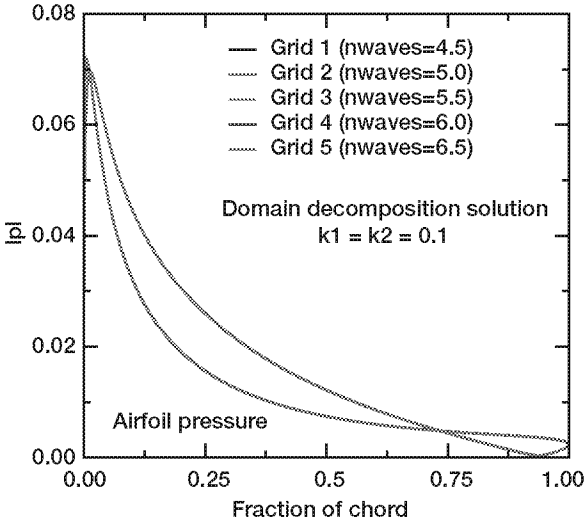

Figure 4.—Grid independent pressure on airfoil surface.

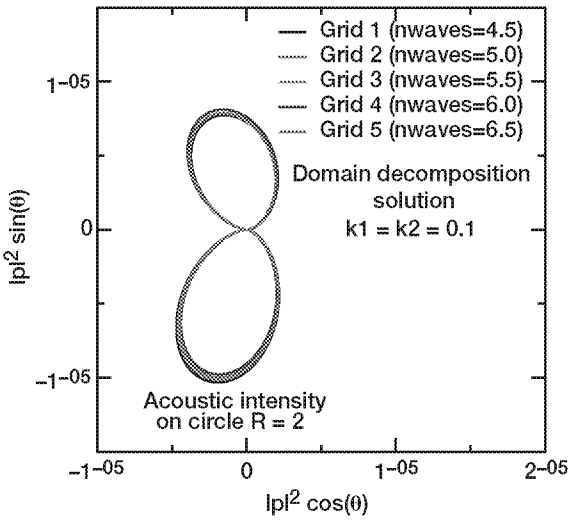

Figure 6.—Effect of far-field boundary location on acoustic intensity.

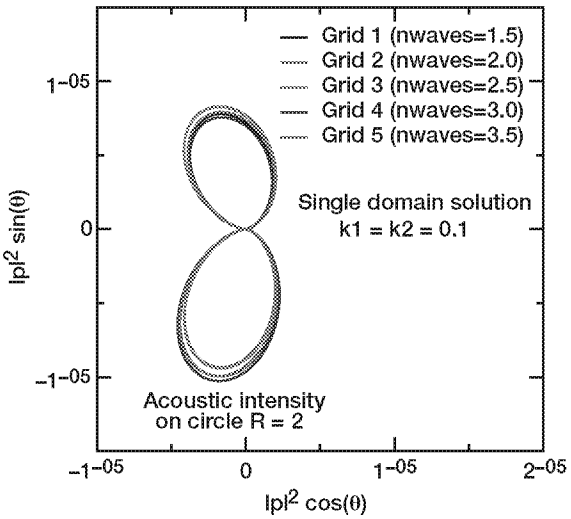

Figure 5.—Effect of far-field boundary location on acoustic intensity.

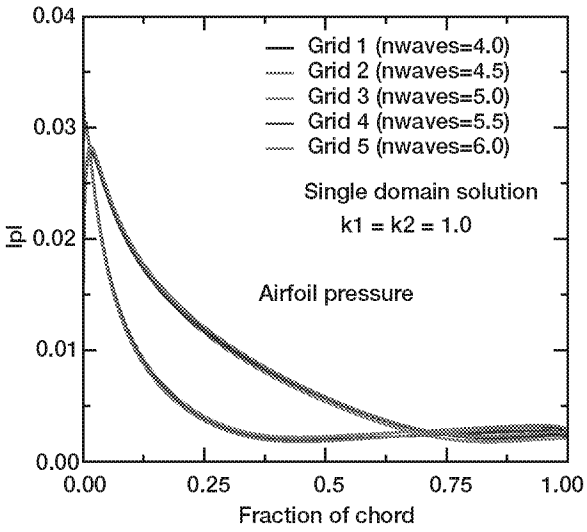

Figure 7.—Effect of far-field boundary location on airfoil pressure.

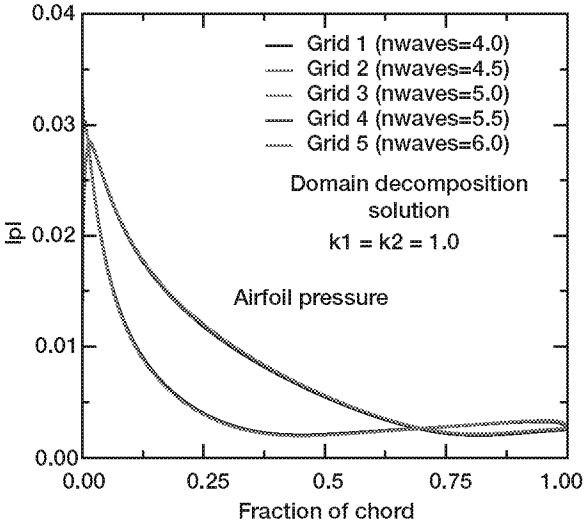

Figure 8.—Improved airfoil solution using domain decomposition approach.

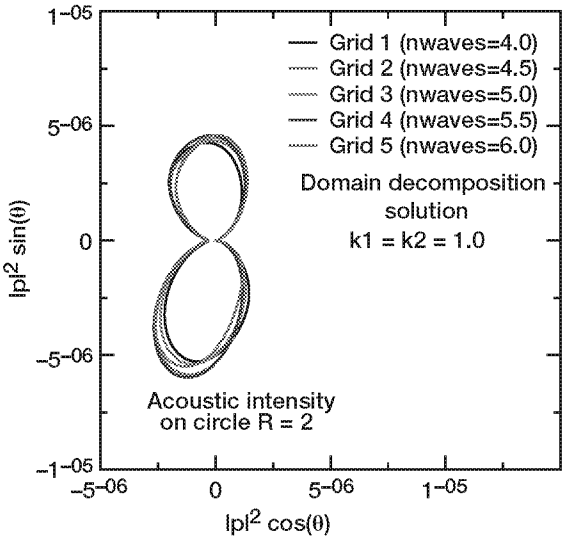

Figure 10.—Improved far-field solution using domain decomposition approach.

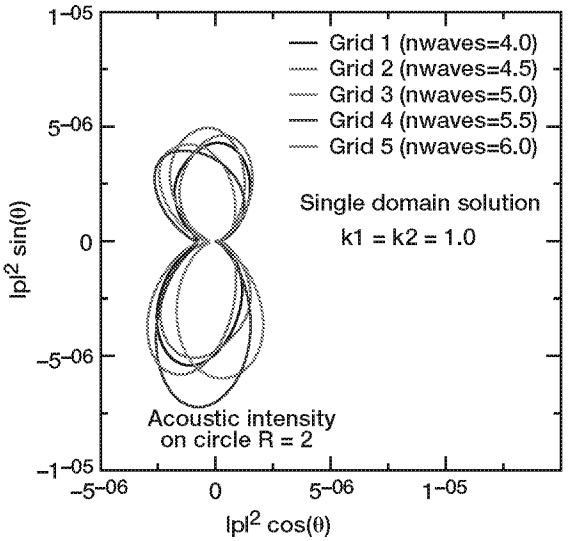

Figure 9.—Effect of far-field boundary location on acoustic intensity.

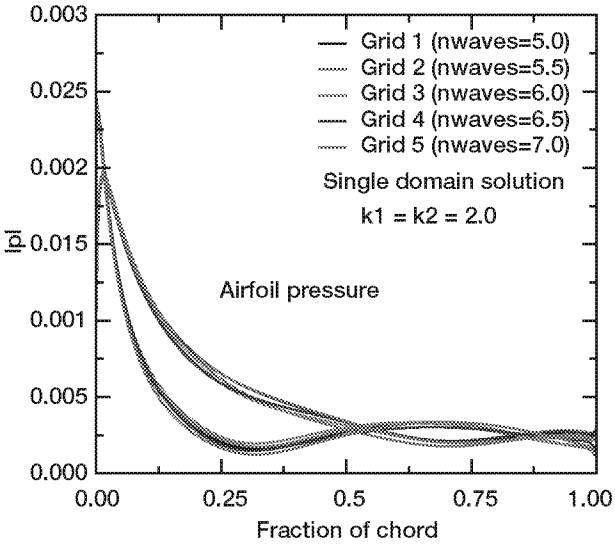

Figure 11.—Effect of far-field boundary location on airfoil pressure.

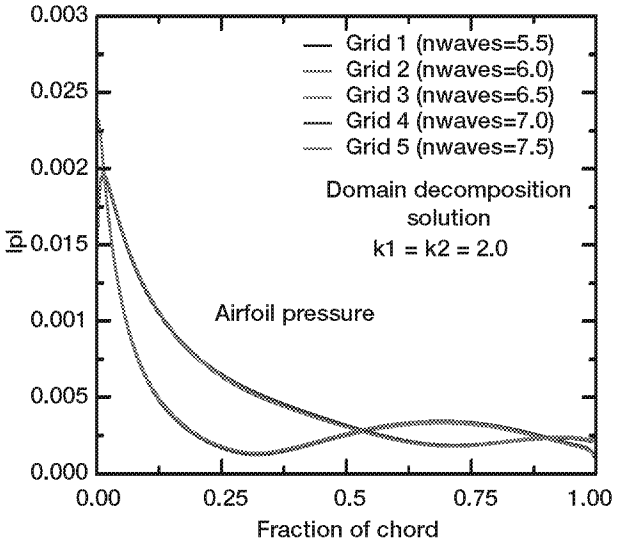

Figure 12.—Improved airfoil solution using domain decomposition approach.

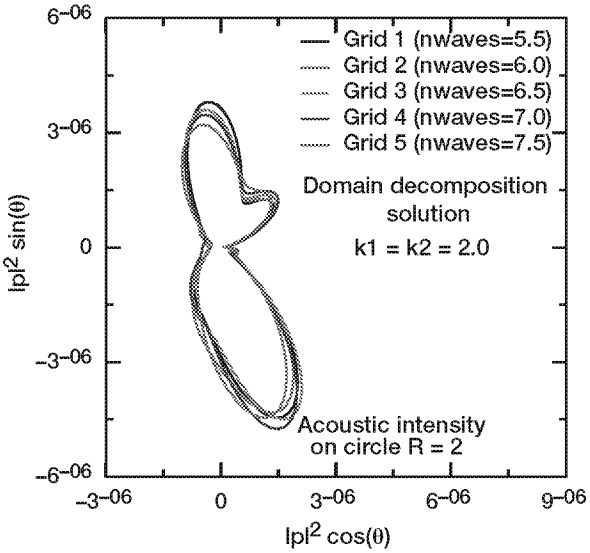

Figure 14.—Improved far-field solution using domain decomposition approach.

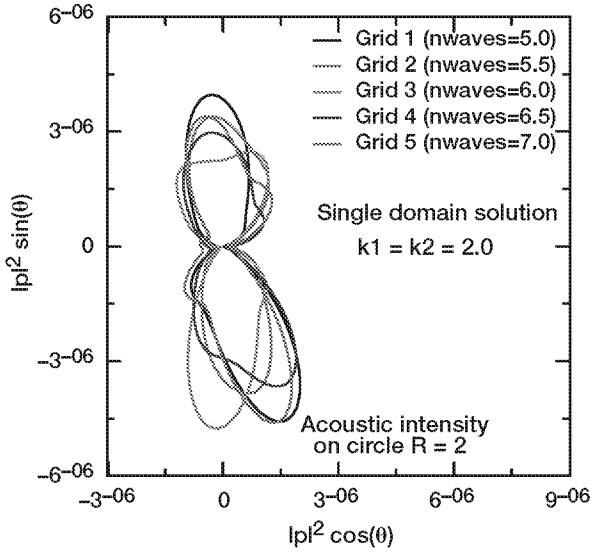

Figure 13.—Effect of far-field boundary location on acoustic intensity.

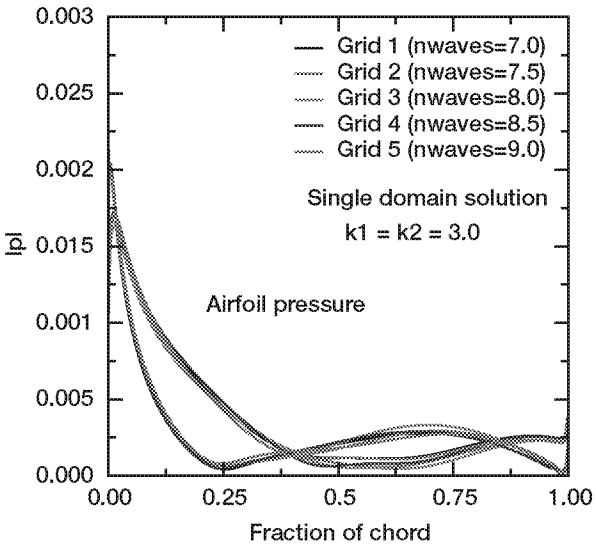

Figure 15.—Effect of far-field boundary location on airfoil pressure.

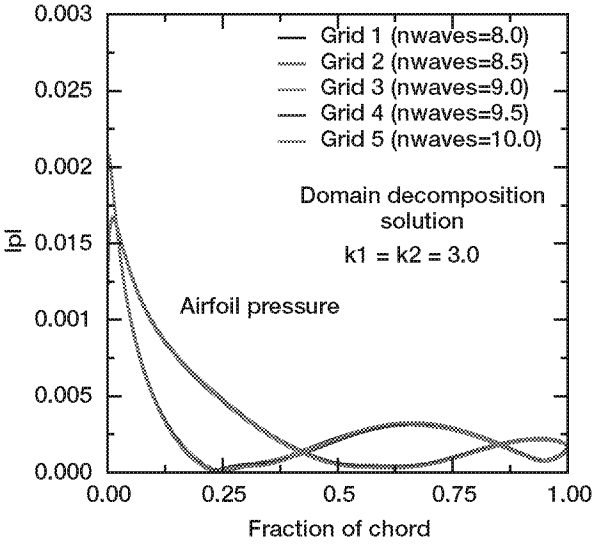

Figure 16.—Improved airfoil solution using domain decomposition approach.

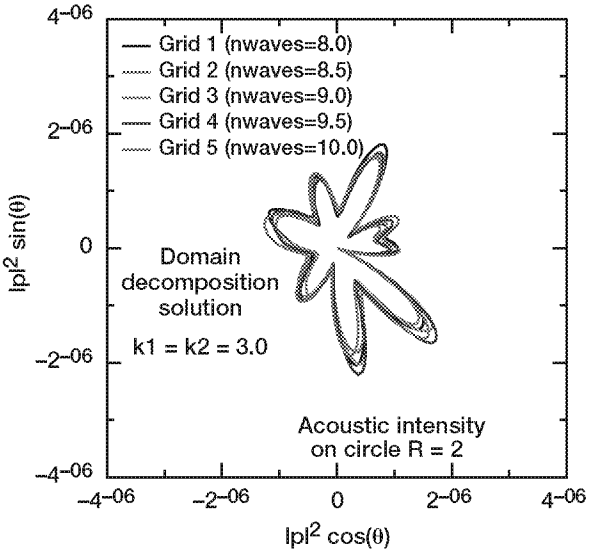

Figure 18.—Improved far-field solution using domain decomposition approach.

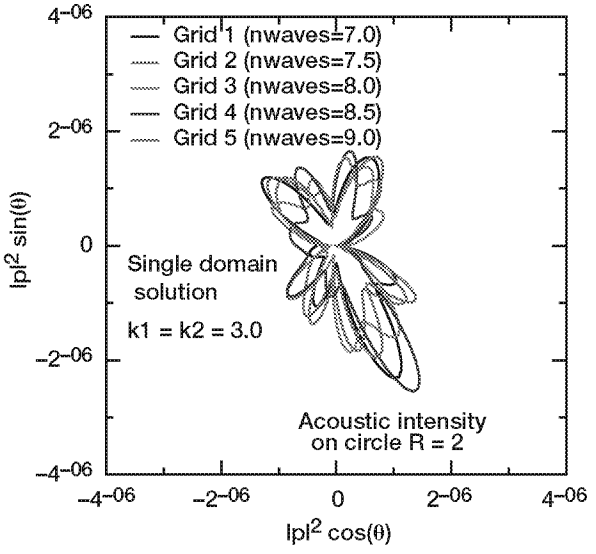

Figure 17.—Effect of far-field boundary location on acoustic intensity.

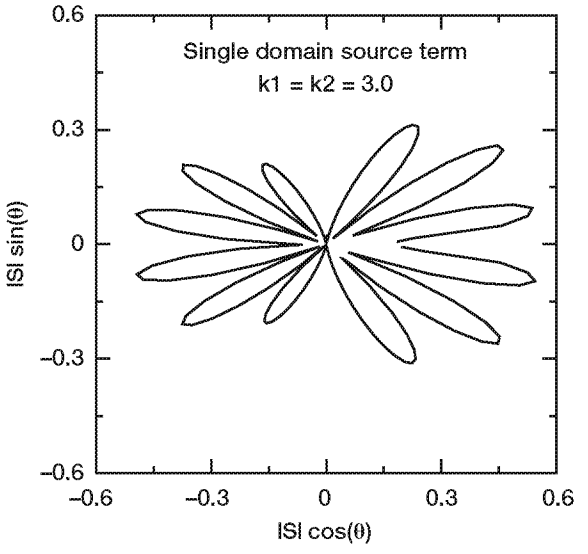

Figure 19.—Polar plot of source term magnitude on a circumferential grid line of radius three chord lengths.

REPORT DOCUMENTATION PAGE

Form Approved
OMB No. 0704-0188

1. AGENCY USE ONLY (*Leave blank*)	2. REPORT DATE	3. REPORT TYPE AND DATES COVERED
	December 2002	Technical Memorandum

4. TITLE AND SUBTITLE

A New Domain Decomposition Approach for the Gust Response Problem

5. FUNDING NUMBERS

WBS–22R–722–96

6. AUTHOR(S)

James R. Scott, Hafiz M. Atassi, and Romeo F. Susan-Resiga

7. PERFORMING ORGANIZATION NAME(S) AND ADDRESS(ES)

National Aeronautics and Space Administration
John H. Glenn Research Center at Lewis Field
Cleveland, Ohio 44135–3191

8. PERFORMING ORGANIZATION REPORT NUMBER

E–13699

9. SPONSORING/MONITORING AGENCY NAME(S) AND ADDRESS(ES)

National Aeronautics and Space Administration
Washington, DC 20546–0001

10. SPONSORING/MONITORING AGENCY REPORT NUMBER

NASA TM—2002-212010
AIAA–2003–0883

11. SUPPLEMENTARY NOTES

Prepared for the 41st Aerospace Sciences Meeting and Exhibit sponsored by the American Institute of Aeronautics and Astronautics, Reno, Nevada, January 6–9, 2003. James R. Scott, NASA Glenn Research Center, and Hafiz M. Atassi and Romeo F. Susan-Resiga, University of Notre Dame, Notre Dame, Indiana 46556. Responsible person, James R. Scott, organization code 5940, 216–433–5863.

12a. DISTRIBUTION/AVAILABILITY STATEMENT

Unclassified - Unlimited
Subject Category: 64 Distribution: Nonstandard

Available electronically at http://gltrs.grc.nasa.gov

This publication is available from the NASA Center for AeroSpace Information, 301–621–0390.

12b. DISTRIBUTION CODE

13. ABSTRACT ***(Maximum 200 words)***

A domain decomposition method is developed for solving the aerodynamic/aeroacoustic problem of an airfoil in a vortical gust. The computational domain is divided into inner and outer regions wherein the governing equations are cast in different forms suitable for accurate computations in each region. Boundary conditions which ensure continuity of pressure and velocity are imposed along the interface separating the two regions. A numerical study is presented for reduced frequencies ranging from 0.1 to 3.0. It is seen that the domain decomposition approach in providing robust and grid independent solutions.

14. SUBJECT TERMS

Computational fluid dynamics; Unsteady aerodynamics; Gusts; Frequency domain analysis; Noise prediction (aircraft); Acoustics

15. NUMBER OF PAGES

17

16. PRICE CODE

17. SECURITY CLASSIFICATION OF REPORT	18. SECURITY CLASSIFICATION OF THIS PAGE	19. SECURITY CLASSIFICATION OF ABSTRACT	20. LIMITATION OF ABSTRACT
Unclassified	Unclassified	Unclassified	